Reliability of Trigonometric Transform-based Multicarrier Scheme

Samah A. Mustafa

Department of Electrical Engineering, College of Engineering, Salahaddin University-Erbil,
Erbil, Kurdistan Region - F.R. Iraq

Abstract– **This work is looking for a new physical layer of a multicarrier wireless communication system to be implemented in low complexity way, resorting to a suitable fast transform. The work presents and assesses a scheme based on Discrete Trigonometric Transform with an appending symmetric redundancy either in each or multiple consecutive transformed blocks. A receiver front-end filter is proposed to enforce a whole symmetry in the channel impulse response. Further, a bank of one tap filter per sub-carrier is applied as an equalizer in the transform domain. The behavior of the transceiver is studied in the context of the practical impairments such as fading channel, carrier frequency offset (CFO), and narrowband interference. Moreover, the performance is evaluated in contrast with the state-of-the-art method by means of computer simulations. It has been found that the new scheme improves the robustness and the reliability of the communication signal, and records lower peak to average power ratio. The study demonstrates that the front-end matched filter effectively performs frequency synchronization to compensate the CFO frequency offset in the received signal.**

Index Terms - **Discrete cosine transform, Discrete fourier transform, Discrete trigonometric transform, Multicarrier modulation, Orthogonal frequency-division multiplexing.**

I. Introduction

Multicarrier (MC) modulation has been applied widely in wireless communication systems due to its high bandwidth efficiency and robustness to multipath distortion. However, its applications have been restricted to scenarios characterized by sufficiently presence of efficient power amplifier and/or slow time variations channel impulse response (CIR). However, the presence of a rapidly time-varying CIR where the time selectivity stems, for example, from the Doppler effect or the oscillators' phase noise, destroys the orthogonality between the sub-carriers and causes Inter-Carrier Interference (ICI)) Ren et al., 2016; Shin et al., 2014). Complex equalization techniques must be employed to cope with the latter effect (Mustafa, 2011).

As the conventional discrete Fourier transform (DFT)-based MC system suffers some performance restrictions and high peak to average power ratio (PAPR), the research community has investigated the use of alternative discrete transforms in MC scheme. Wavelet transform in orthogonal frequency-division multiplexing (OFDM) system is studied by Lee and Ryu, 2017, Sirvi and Tharani, 2016, and Suma and Narasimhan, 2018, to replace the DFT in the modulator/demodulator implementation. Another method using the discrete cosine transform (DCT) for MC communication schemes has been studied by Al-Dhahir and Minn, 2006; Cruz-Roldan et al., 2012; Chafii et al. 2016; Feifei et al., 2008; and He et al., 2018). DCT-based scheme has been found as less sensitive to carrier offset. Furthermore, it is a real transform, which can avoid the in-phase/quadrature phase imbalance when the data mapping is real (Feifei et al., 2008).

Many techniques have been investigated to reduce the PAPR in OFDM signal. Wang et al. (2010) proposed a joint companding transform and Hadamard transform method that would introduce high adjacent channel interference with spectrum regrowth. Two different approaches are pointed out in Barsanti and Larue, 2011, active constellation extension method and the reserve carrier algorithm. A precoding method is applied by Hasan (2014) using the decorrelation property of complex Vandermonde matrix. Combination of higher order partitioned partial transmitted sequence along with Bose Chaudhuri-Hocquenghem Code has been proposed by Gupta and Jain (2015). However, these techniques add complexity and consume more resources.

In this paper, two new MC schemes are presented that retain the advantage of the DFT-OFDM of the one-tap filter in the transform domain and reduce the PAPR and the sensitivity to carrier offset substantially. The DFT is replaced by DCT and the well-known discrete trigonometric transform (DTT), namely the DCT and discrete sine transform (DST)

ARO-The Scientific Journal of Koya University
Volume VI, No.2 (2018), Article ID: ARO.10312, 7 pages
DOI: 10.14500/aro.10312
Received 07 October 2017; Accepted: 18 October 2018
Regular research paper: Published 22 December 2018
Corresponding author's e-mail: samah.mustafa@su.edu.krd

 http://dx.doi.org/10.14500/aro.10312

in this work. DCT and DST are linear Fourier-related transformation similar to the DFT, but using a purely real matrix. DCT/DST is equivalent to the real/imaginary parts of a DFT of roughly twice the length, operating on real data with even/odd symmetry. In DTT-based MC scheme, the DTTs are interspersed in the modulator stage: The DCT coefficients are transmitted on the even subcarriers and the DST coefficients are transmitted on the odd subcarriers.

Pseudo-noise (PN) sequence is used to append symmetric redundancy either in each or multiple consecutive transformed blocks. Many simulations have been carried to outline and assess the schemes in the presence of various channel impairments. The receiver employs the channel estimation based on a matched filter approach: It is used to estimate the random attenuation and phase shift of the fading channel and train the decision to adjust the received signal with amplitude and phase recover.

In Section II, discrete-time transmitter and receiver models based on DCT and DTT schemes are proposed. Section III represents the processing to reconstruct the original data through one-tap per sub-carrier. Simulation results and some further discussions of the error performance over different channel parameters are presented in section IV. Finally, Section V concludes the results.

II. DTT in MC Scheme

DCT and DST are orthogonal linear trigonometric transform (Strang, 1999) and each can be implemented by a fast transform that does not require an extensive increase of system complexity. Moreover, they are well-known to have excellent spectral compaction and energy concentration properties which prevent excessive leakage into the adjacent bands (Bouzegzi et al., 2008). They are robust in the presence of ICI.

A. Transmitter Scheme

A linear modulation scheme is presented in Fig. 1. The transmitted signal is obtained by modulating a set of filters $\psi^i(t)$. The filters are chosen as length T rectangular pulse with a suitable multiplexing in the frequency domain as in the uniform filter-bank approach, and based on the discrete transform of interest. We resort to a discrete-time model where $n \triangleq nT_s \triangleq nT/v$ (T_s is the sampling interval and v is the oversampling factor). The transmitted signal is given by:

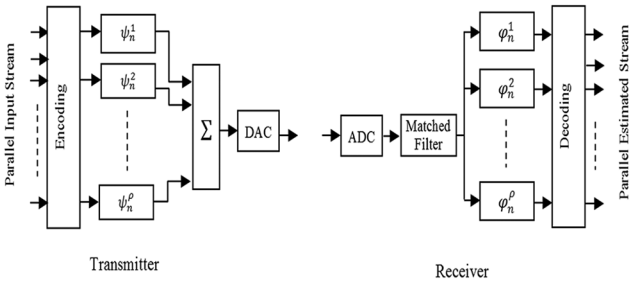

Fig. 1. Discrete time filter bank transceiver.

$$x(t)=\sum_k \sum_{i=1}^{\rho} \xi^i{}_k \sum_n \psi_n{}^i \, rect\left(\frac{t-kT-nT_s}{T_s}\right) \tag{1}$$

A sequence of complex serial information symbols is given by a generic user at a rate ρ/T and is converted into group of low rate parallel streams; each modulates a mutually orthogonal sub-carrier individually. ρ being an integer design parameter and T is transmitted block time period. The symbols are zero-mean independent random variables (r.v.s) belonging to a given complex constellation. i denotes subcarrier index or symbol position inside a block which is identified by an index k. $\psi^i{}_n$ denotes the set of oversampled version of the filters. The rectangular function plays the role of digital-to-analog converters. However, slow decay of rectangular pulse in the frequency domain leads to experience strong interference.

In a transmitter scheme employing DCT as an alternative to DFT, transmitter filters are obtained by modulating the rectangular pulse by cosine functions. The orthogonal DCT is classified into many different types with slightly different even/odd boundary conditions at the two ends of the matrix. In this work, the filters are given by

$$\psi_n{}^i = \frac{1}{\sqrt{\rho}} \sum_{i=1}^{\rho} \alpha_i \cos\left(\frac{\pi(2n+1)(i-1)T_s\Delta f}{\rho}\right) \tag{2}$$

$$\alpha_i = \begin{cases} 1 & i=1 \\ \sqrt{2} & 2 \le i \le \rho \end{cases}$$

$1/\sqrt{\rho}$ is a normalization term and Δf is the frequency separation between the adjacent subcarriers. For each transmitted block, the transmitter and receiver carry out a ρ-IDCT and ρ-DCT, respectively. DCT transform operators map a ρ-size real sequence into another ρ-size real sequence, and hence parsed in-phase, and quadrature components of complex data word must be used in each sub-channel individually. Unlike it, the complex information block is forced to be conjugated symmetric to ensure a real-valued inverse DFT output at the transmitter. When real-valued modulation formats, for instance, BPSK or PAM are used, DCT-based scheme doubles the spectral efficiency compared to that in the DFT-based scheme.

This work also studies another transmitter scheme based on both DCT and DST to build DTT-based MC scheme. The rectangular pulse is modulated by a cosine function for the even index subcarriers and by sine function for the odd index subcarriers.

$$\psi_n{}^i = \begin{cases} \frac{1}{\sqrt{\rho}} \sum_{i=1}^{\rho} \alpha_i \cos\left(\frac{\pi(2n+1)(i-1)T_s\Delta f}{\rho}\right) & if\ i\ even \\ \frac{1}{\sqrt{\rho}} \sum_{i=1}^{\rho} \beta_i \sin\left(\frac{\pi(2n+1)iT_s\Delta f}{\rho}\right) & if\ i\ odd \end{cases} \tag{3}$$

Where α_i as given before $\alpha_i = \begin{cases} 1 & i=1 \\ \sqrt{2} & 2 \le i \le \rho \end{cases}$

and $\beta_i = \begin{cases} 1 & i=\rho \\ \sqrt{2} & 1 \le i \le \rho-1 \end{cases}$

Γ output blocks in either DCT or DTT scheme are serialized and encapsulated in a frame to get a vector X of ($\Gamma v\rho$) elements. $v\rho$ represents number of samples in each block. To leverage the performance and afford the delay spread over wireless channel, symmetric redundancy (prefix and suffix) each of length β is successively arranged to form the first block in each frame. In this work, PN is inserted as the redundancy in the transmitted sequence. The redundancy sequence strengthens the transmission especially over a channel of long impulse response and restricts the transmission spectral efficiency. The spectral efficiency is the amount of pre-code bits that can be loaded on a time-frequency region characterized by a unitary bandwidth and time slot.

It is well known; there is a tradeoff between the spectral efficiency and the error performance, such that lower number of encapsulated blocks Γ in a frame enhances the performance but with sacrificing in the transmission rate and the spectral efficiency. Compared to the conventional scheme based on DFT, DCT or DTT-based scheme records a gain of 1.19 bps/Hz in the spectral efficiency if the transmitter is considered to transmit a frame of four independent output blocks. A gain of 2.38 bps/Hz is obtained using real signaling to encode the subcarriers.

B. Receiver Scheme

After transmission over a noisy fading channel, the discrete time received signal is given by the convolution of the transmit signal $x(t)$ and the time-varying CIR $\lambda(t)$ as:

$$\Upsilon(t)=\int_{-\infty}^{+\infty}\lambda(\tau)x(t-\tau)d\tau+\eta(t) \quad (4)$$

$\lambda(t)$ is zero-mean Gaussian random process, and η is a complex white Gaussian process. At the reception side, a front end pre-matched filter is present to use a fraction signal of each frame to estimate the frame timing and carrier frequency offset (CFO). The estimated information symbol $\dot{\xi}_m^i$ at a subcarrier, i in a processed block m can be found as:

$$\dot{\xi}_m^i=\sum_n \varphi_n^i \int_{-\infty}^{+\infty}(\Upsilon(t)*\text{Ϭ}(t))\,rect\left(\frac{t-mT-nT_s}{T_s}\right)dt \quad (5)$$

The received signal is processed by a bank of ρ filters φ_n^i DCT and DST are orthogonal linear transform and hereby $\varphi_n^i=\psi_n^i$. Ϭ(t) denotes the impulse response of the pre-matched filter. The rectangular function here plays the role of analog-to-digital conversion.

In traditional synchronization approaches, one estimate suffers from a performance degradation caused by estimation error of the other. In this work, a matched filter is used to exploit the received training signal for joint coarse time and frequency synchronization too: To estimate the symbol timing and CFO. Fig. 2 shows a block diagram of the matched filter. The matched filter coefficients are $\varsigma_1\ \varsigma_2\ \ldots\ \varsigma_\beta$, and ς_k is the chip value of the redundancy in the transmitted sequence. The symbol timing and carrier offset can be achieved by searching for the correlation peak in the matched filter output.

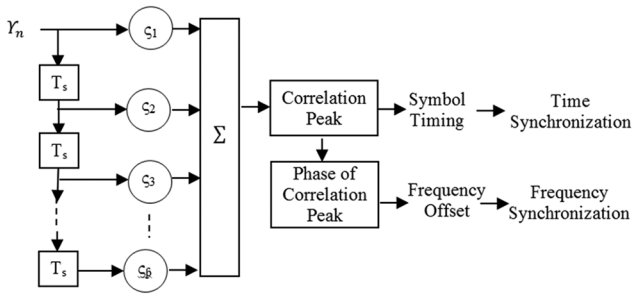

Fig. 2. Block diagram of the pre-matched filter.

The coherent detection of PN synchronization sequence consists of a coherent accumulation of cross-correlations sub-channels by means of the matched filter. It improves frequency acquisition and reduces the miss on a channel with a sufficiently wide coherence bandwidth. The method is proposed in the DFT-based system and presented with detailed derivation in Lin, 2008.

The next section addresses the processing in DCT and DTT-based schemes under which the original data can be reconstructed through one-tap per sub-carrier transform domain equalizer at the receiver. However, the main drawback of DCT or DTT-based system with respect to the conventional DFT-based scheme is the need for a pre-filter at the receiver to make the CIR symmetric.

III. Channel Equalization in Trigonometric Transform-Based Scheme

This section portrays matrix representation of signal processing in the scheme. The processing is demanded to robust the transmission performance and mitigate the intersymbol interference ISI. Let us consider a CIR given as β filter taps.

$$\underline{\lambda}=[\lambda_o,\lambda_1,\ldots,\lambda_\beta]^T \quad (6)$$

$(.)^T$ is the transposition operator. The front-end filter at the reception side as in Al-Dhahir and Minn, 2006, is used to present symmetry in the channel filter as:

$$\underline{\lambda}=[\lambda_\beta,\ldots,\lambda_1,\lambda_o,\lambda_1,\ldots,\lambda_\beta]^T \quad (7)$$

If a transformed block is given as:

$$\underline{x}=[\ x_o,x_1,\ldots,x_{\beta-1}\ ] \quad (8)$$

To minimize the probability of interblock interference, each can be extended with $\underline{x}$ appending symmetric redundancy each of length β.

$$\underline{\dot{x}}=[\ x_\beta,x_{\beta-1},\ldots,x_1,x_o,x_1,\ldots, x_\rho,x_{\rho-1},x_{\rho-2},\ldots,x_{\rho-\beta-1}] \quad (9)$$

$$\underline{\dot{x}}=\begin{bmatrix}0_{(p+2\beta)X1} & \dfrac{G_{\beta X\beta}}{0_{(p+\beta)X\beta}} & 0_{(p+2\beta)X(p-\beta-1)}\end{bmatrix}\underline{x}^T+ [0_{1X\beta}\quad \underline{x}\quad 0_{1X\beta}]^T+ \begin{bmatrix}0_{(p+2\beta)X(p-\beta-1)} & \dfrac{0_{(p+\beta)X\beta}}{G_{\beta X\beta}} & 0_{(p+2\beta)X1}\end{bmatrix}\underline{x}^T \quad (10)$$

 http://dx.doi.org/10.14500/aro.10312

0_{MXN} denotes a matrix of zero elements. The sub-matrix $G_{\beta X\beta}$ is composed of a single zero column and a Henkel matrix where each ascending skew-diagonal from left to right is constant. In this work, all elements are zeros except, $g_{i,\beta-i+1}=1$ and is used to find the prefix and suffix for a transformed block.

$$G=\begin{bmatrix} 0 & \dots & \dots & \dots & 1 \\ \vdots & \ddots & 0 & 1 & 0 \\ \vdots & \ddots & 1 & 0 & 0 \\ \vdots & \ddots & \ddots & \ddots & \vdots \\ 1 & 0 & \dots & \dots & 0 \end{bmatrix} \tag{11}$$

$\frac{G_{\beta X\beta}}{0_{(p+\beta)X\beta}}$ extends the G matrix by inserting ρ + β rows of zero elements. Matrix representation of Eq. (4) using ΄H is a Toeplitz matrix in which each descending diagonal from left to right is constant, and is given as:

$$\underline{y}={}'H\underline{x}^{T}+n \tag{12}$$

Based on (2), the delivered signal block can rewritten as:

$$\underline{y}={}'H\begin{bmatrix} G_l \\ I_{\rho X\rho} \\ G_r \end{bmatrix}\underline{x}^{T}+\eta \tag{13}$$

$$'\ddot{H}=\begin{bmatrix} \lambda_\beta & \dots & \lambda_1 & \lambda_o & \dots & \lambda_\beta & 0 & \dots & 0 & \dots & 0 \\ 0 & \lambda_\beta & \ddots & \lambda_1 & \lambda_o & \ddots & \ddots & \ddots & \ddots & \ddots & \vdots \\ \vdots & \ddots & \ddots & \ddots & \ddots & \ddots & \ddots & \ddots & 0 & \ddots & 0 \\ 0 & \ddots & 0 & \lambda_\beta & 0 & \ddots & \ddots & 0 & \lambda_\beta & \cdots & 0 \\ \vdots & \ddots & \ddots & \ddots & \ddots & \ddots & \ddots & \ddots & \ddots & \ddots & \vdots \\ 0 & \dots & 0 & 0 & \dots & \lambda_\beta & \dots & \lambda_o & \lambda_1 & \dots & \lambda_\beta \end{bmatrix}$$
$$\begin{bmatrix} 0_{\beta X1} & G_{\beta X\beta} & 0_{\beta X(p-\beta-1)} \\ & I_{pXp} & \\ 0_{\beta X(p-\beta-1)} & G_{\beta X\beta} & 0_{pX1} \end{bmatrix} \tag{14}$$

$'\ddot{H}_{\rho X\rho}$ is a symmetric circular matrix where $\lambda_{i,j}=\lambda_{\rho+1-i,\rho+1-j}$. If β=3 & ρ=5, $'\ddot{H}$ is given as:

$$'\ddot{H}=\begin{bmatrix} \lambda_o & 2\lambda_1 & 2\lambda_2 & 2\lambda_3 & 0 \\ \lambda_1 & \lambda_o+\lambda_2 & \lambda_1+\lambda_3 & \lambda_2 & \lambda_3 \\ \lambda_2 & \lambda_1+\lambda_3 & \lambda_o & \lambda_1+\lambda_3 & \lambda_2 \\ \lambda_3 & \lambda_2 & \lambda_1+\lambda_3 & \lambda_o+\lambda_2 & \lambda_1 \\ 0 & 2\lambda_3 & 2\lambda_2 & 2\lambda_1 & \lambda_o \end{bmatrix} \tag{15}$$

$'\ddot{H}$ can be diagonalized by applying inverse and forward DTT: C^{-1} and C respectively. DTT is given in Eq (2).

$$\begin{aligned} \underline{y} &= C^{-1}C'\ddot{H}C^{-1}C\underline{x}^{T}+\eta \\ &= C^{-1}ĐC\,\underline{x}^{T}+\eta \end{aligned} \tag{16}$$

Đ contains the eigenvalues of $'\ddot{H}$ which are DTT of $\tilde{\underline{\lambda}}$.

By sending pilot block $\underline{x_\beta}$, the channel state information CSI presented in $\tilde{\underline{\lambda}}$ can be estimated by the scalar division of diagonal matrix elements by $C\underline{x_\beta}$ followed by inverse DTT. A bank of one tap filter per sub-carrier is applied as an equalizer in the transform domain. The efficacy of the filter rises up when the noise in the delivered signal is alleviated.

IV. Simulation Study

The behavior of the proposed approach is studied in the context of practical impairments such as non-linear distortion, fading channel, and CFO, and in the presence of narrowband interference. Further, the performance of the proposed approach is evaluated in contrast with the state-of-the-art system by means of computer simulations.

Information bits are grouped and mapped using either differential phase shift keying (DPSK) or quadrature amplitude modulation (QAM) with a constellation size of 16 states. With Fourier transformation, the conjugate symmetry condition is imposed in the system under the same transformation size of 256 to provide a fairest comparison possible. The results are averaged over a number of independent iterations of the process.

A. Fading Channel

The received samples at time intervals nT_s can be expressed as:

$$\Upsilon_n=\partial_n\, e^{j2\pi\Omega ni/\rho}x_{n-l}+\eta_n \tag{17}$$

ι is the unknown delay time in the transmitted sample x. Ω_n denotes the CFO in a sub-carrier spacing centered at a normalized subcarrier frequency is i/ρ. ∂_i is the time varying i^{th} sub-channel fade which has Rayleigh distributed envelope and uniformly distributed phase. ε represents the CFO and causes phase ambiguity. It can be expressed as a complex Gaussian random process with the autocorrelation function as given by:

$$E\left[\partial_{i1}\partial_{i2}^{*}\right]=J_o(2\pi f_D\left|i_1-i_2\right|\frac{T}{\rho}) \tag{18}$$

E[·] denotes the statistical expectation operation, and $J_o(\cdot)$ is the zeroth-order Bessel function of the first kind. f_D is the maximum Doppler frequency caused directly by relative motion.

Flat fading channel

The coherence bandwidth measures the separation in frequency after which two signals will experience uncorrelated fading. In flat fading, the coherence bandwidth of the channel is larger than the bandwidth of the signal. Therefore, all frequency components of the signal will experience the same magnitude of fading ∂. The channel can be expressed as a single complex filter tap. The channel gain is random with a significant probability that the channel is in a deep fade, that is, $|\lambda|^2 < N_o/E$. The probability of this event is roughly defined in Tse and Viswanath, 2005, as:

$$P(\left|\lambda\right|^2<\frac{N_o}{E})\approx\frac{N_o}{E} \tag{19}$$

E/N_o is the average received signal energy-to-noise energy ratio per complex symbol time. To assess the performance of

DCT and DTT-based MC schemes over fading channel, the error curves are examined as a function of signal energy-to-noise E/N_o. The results are compared with the corresponding performance of DFT-based scheme. Non-coherent communication is considered here where the receivers have no prior knowledge of the channel. Fig. 3 shows the performance of different encoded sub-carriers where the new proposed schemes approach the linear transmission. The distortion arose from a fading channel can be compensated by increasing E/N_o. As depicted, DPSK signals in all the investigated MC systems perform well depending on the phase tracking of the decoder: DPSK modulated sub-carriers track and predict the channel response by itself. It is clearly observed that QAM modulated sub-carriers behave better in DCT and DTT-based schemes, while in the conventional scheme based on DFT they result in higher error rates.

Slow fading channel

By the assumption of transmission over a slow fading channel, the coherence time of the channel is large relative to the delay constraint of the channel. The amplitude and phase change imposed by the channel can be considered roughly constant over the period of a frame. Slow fading can be caused by events such as shadowing, where a large obstruction such as a hill or large building obscures the signal path. In this regime, the number of encapsulated symbols in a frame gets higher and subsequently increases the bandwidth efficiency.

Extra simulations have been carried out to investigate the performance of coherent detection in the new schemes over a slow fading channel. For a coherent communication, the receiver estimates the channel state information CSI and adaptively equalizes the delivered symbols to compensate the fade impairments. The CSI in each coherence time is estimated, and the weight of each tap in the equalizer is trained by pilot PN sequence in DCT and DTT-based frames.

Previous works have addressed the problem of obtaining a condition under which the original data can be reconstructed through one-tap per sub-carrier equalizer in DCT-based MC scheme. Following the same approach in Domınguez-Jimenez et al., 2011, to correct the fade impairments, a suffix and a prefix are inserted in the transmitted DCT-symbol. Moreover, a front-end pre-filter is employed in the receiver to force symmetry in the CIR.

Fig. 4 graphs the simulated error rates as a function of in E/N_o the received signal. The blind detection process with no channel state information results in an irreducible error. A bank of scalars as a channel equalizer at the receiver results in better performance. DTT scheme records an improvement in the error performance over both DFT and DCT schemes, where a slight difference in the error rates has been found between the latter two schemes.

B. CFO and narrowband interference

The DFT-based scheme offers reliable, effective transmission; however, it is far more vulnerable to CFO that can cause a high bit error rate and performance degradation due to ICI. In DCT and DTT-based schemes, one extension interval is used for each frame of a number of consecutive output blocks. Common estimates of the symbol timing and the frequency offset can be

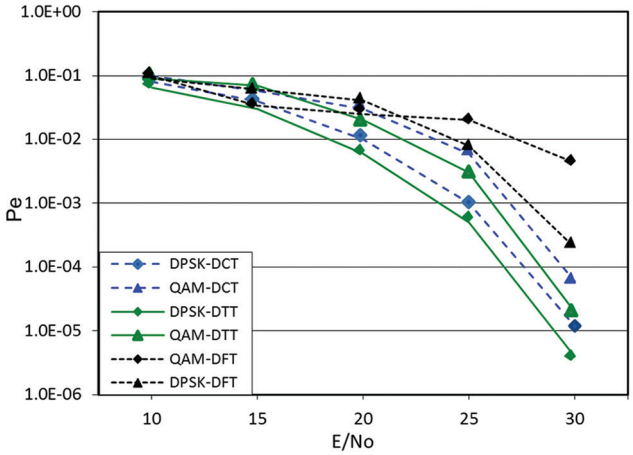

Fig. 3. Error performance of different multicarrier schemes over flat fading channel.

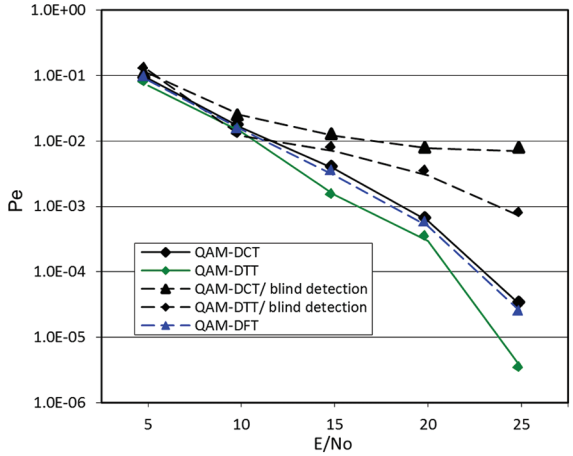

Fig. 4. Error performance of different multicarrier schemes over a slow fading channel. The receiver is either based on blind detection or the estimated CSI.

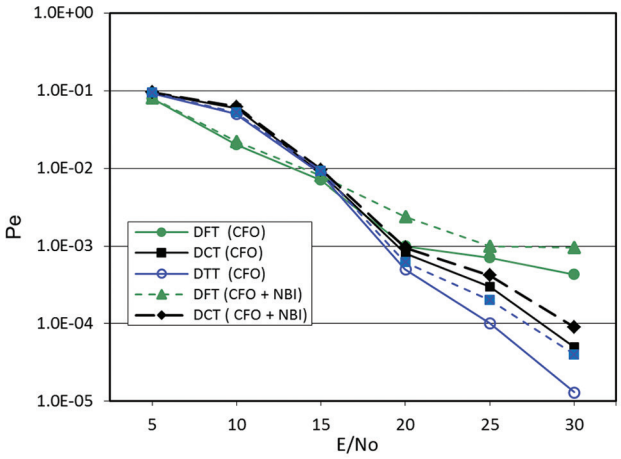

Fig. 5. Error performance of multicarrier schemes in the presence of CFO and a narrowband interference.

http://dx.doi.org/10.14500/aro.10312

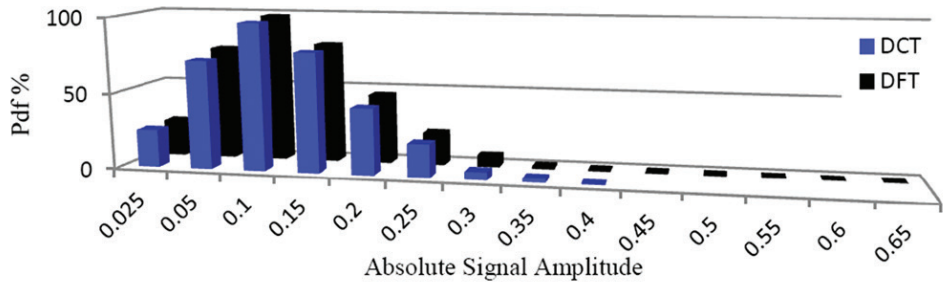

Fig. 6. Probability distributions function of the absolute amplitude of DCT - and DFT-based transformed blocks.

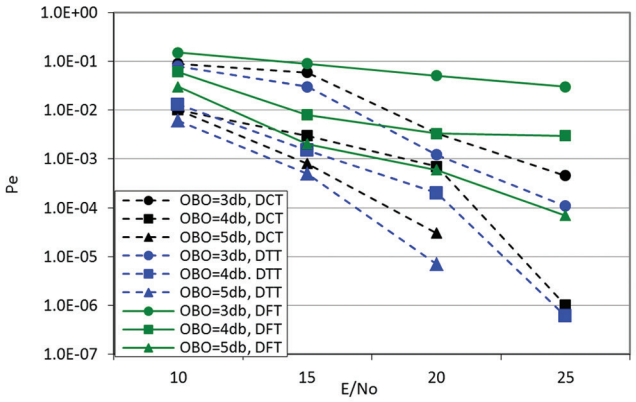

Fig. 7. Error performance of multicarrier schemes with the presence of non-linear distortion.

evaluated jointly when a peak is found in the correlator output. It is proved that DCT and DTT schemes are more robust in the presence of CFO and a narrowband interference NBI. Fig. 5 graphs the error rates in the presence of CFO of 0.13 in the delivered signal over an additive white Gaussian noise channel, and interference as a continuous wave signal.

C.Non-linear distortion

In this section, the time domain transformed amplitude in the conventional OFDM and the proposed systems are analyzed as depicted in Fig. 6. The probability density function (PDF) depends on the probability of occurrence of each discrete sample level. The distribution of MC signal with 512 sub-carriers and 16-QAM is founded where the amplitude ε has Rayleigh distribution with PDF given by:

$$(\varepsilon;\sigma)=\begin{cases}-e^{-\varepsilon^2/(2\sigma^2)} & if\ \varepsilon\geq 0\\ 0 & elsewhere\end{cases} \quad (20)$$

σ is the scaling parameter. For Rayleigh distribution, as seen the signal levels around the mean value have higher probability than other levels, whereas the occurrence of higher signal levels has smaller probability. It is reasonable to cast a way to change the statistic of the amplitude for the benefit of PAPR reduction. Notice that PAPR is a r.v. for each transmitted block, and, generally, is given as the ratio of the maximum instantaneous power in the block to the average block power E $[x_i|^2]$.

$$PAPR\{x_i^k\}=\frac{\max_{1\leq i\leq p}|x_i|^2}{E[|x_i|^2]} \quad (21)$$

High PAPR in OFDM signal has a detrimental effect on the performance: The power amplifier clips the transmitted signal and results in non-linear distortion. Based on number of independent runs for the schemes, the proposed system is found to preserve the average power and a reduction of about 4.5 db in the peak power and 1.6 db in the PAPR compared to the conventional OFDM scheme.

The BER performance when the system encompasses power amplifier within its structure is presented in this section. Non-linear power amplifier is applied with AM/AM response of clipping scheme at the saturation point at three different output back off (OBO); 3, 4, and 5 dB. OBO is defined as the ratio of the maximum possible amplifier output power to the average output power. The error performance of the new MC scheme based on DCT and DTT has been compared with the corresponding performance of the traditional Fourier-based MC scheme (Fig.7) over a noisy channel. The complex-valued noise is assumed to be independent and identically distributed, zero-mean white Gaussian noise. Its variance is equal to N_o per real dimension.

In the traditional MC scheme, low OBO generates an almost flattened error curve indicating saturation of the power amplifier. These results can be directly compared with the results of the new schemes. It is found that the simulated performance approaches the linear transmission due to the overall net improvement in the PAPR. However, lower OBO causes non-linear distortion that diverge the performance from the linear case. The PAPR in DTT blocks and the performance of DTT-based scheme with existence of OBO is quite similar to that presented for the DCT-based scheme.

V. Conclusion

In this work, two MC schemes based on trigonometric transform are introduced. In the first scheme, the subcarriers are DCT transformed whereas the subcarriers are either DCT or DST transformed based on their index in the second scheme. Extensive simulations have been carried out to study the

performance of DCT and DTT schemes compared to that of the traditional DFT-based scheme. The performance is investigated over flat fading and slow fading channels, where DCT and DTT schemes show better error performance at high E/N_o.

In the proposed scheme appending symmetric redundancy (as prefix and suffix) in the transmit block and symmetric equivalent CIR, implies the use of a bank of scalars in the corresponding trigonometric transform domain to equalize the channel response. The study is carried by several simulations in wireless communication scenarios, considering the presence of CFO and multipath channel. The results indicate that trigonometric-based systems outperform the conventional scheme based on the Fourier transform.

Our simulation results showed a reduction in the PAPR and leverage in bandwidth efficiency. Performance improvement in the presence of non-linear distortion for the case of the proposed system has been achieved in comparison with that for the conventional OFDM systems.

References

Al-Dhahir, N., and Minn, H., 2006. Optimum CDT-based multicarrier transceivers for frequency-selective channels. *IEEE Transaction on Communications*, 54(5), pp.911-921.

Barsanti, R.J., and Larue, J., 2011. Peak to average power ratio reduction for digital video broadcast T2. *Southeastcon IEEE*, 2011, pp.117-121.

Bouzegzi, A., Ciblat, P., and Jallon, P., 2008. *Matched Filter Based Algorithm for Blind Recognition of OFDM Systems*. 68th IEEE Vehicular Technology Conference, pp.1-5.

Chafii, M., Palicot, J., Gribonval, R., and Bader, F., 2016. A necessary condition for waveforms with better papr than OFDM. *IEEE Transaction on Communication*, 64(8), pp.3395-3405.

Cruz-Roldan, F., Dominguez-Jimenez, M.E., Vidal, G.S., Amo-Lopez, P., Blanco-Velasco, M., and Bravo-Santos, A., 2012. On the use of discrete cosine transforms for multicarrier communications. *IEEE Transaction on Signal Processing,* 60, pp.6085-6090.

Domınguez-Jimenez, M., Sansigre, G., Amo-Lopez, P., and Cruz-Roldan, F., 2011. *DCT Type-III for Multicarrier Modulation*. In: Proceeding 19th European Signal Processing Conference (EUSIPCO 2011). Barcelona, Spain: pp.1593-1597, August- September, 2011.

Feifei, G., Tao, C., Nallanathan, A., and Tellambura, A., 2008. Maximum likelihood based estimation of frequency and phase offset in DCT OFDM systems under non-circular transmissions: Algorithms, analysis and comparisons. *IEEE Transaction on Communication,* 56(9), pp.1425-1429.

Gupta, P., and Jain, S., 2015. *Peak to Average Power Ratio Reduction in OFDM Using Higher Order Partitioned PTS Sequence and Bose Chaudhuri Hocquenghem Codes*. In: Proceeding International Conference on Signal Processing and Communication Engineering SPACES; 2015.

Hasan, M., 2014. A novel CVM precoding scheme for PAPR reduction in OFDM transmissions. *Wireless Networks*, 20(6), pp.1573-1581.

He, C., Zhang, L., Mao, J., Cao, A., Xiao, P., and Imran, M., 2018. Performance analysis and optimization of dct-based multicarrier system on frequency-selective fading channels. *IEEE Access*, 6, pp.13075-13089.

Lee, J., and Ryu, H.G., 2017. *Performance comparison between wavelet-based OFDM system and iFFT-based OFDM system*. In: Proceeding International Conference on Information and Communication Technology Convergence ICTC; 2017.

Lin, J.C., 2006. Coarse frequency-offset acquisition via subcarrier differential detection for OFDM communications. *IEEE Transactions on Communications*, 54(8), pp.1415-1426.

Mustafa, S., Hikmat, V., Shekha, S. 2011. *Wavelet Filter Bank-Based Non Uniform Multi-tone Transceiver for Digital Subscriber Line*. In: Proceeding IEEE 11th International Conference on Computer and Information Technology, pp.197-203.

Ren, X., Tao, M., Chen, W. 2016. Compressed channel estimation with position-based ICI elimination for high-mobility SIMO-OFDM systems. *IEEE Transactions on Vehicular Technology*, 65(8), pp.6204-6216.

Shin, W.J., Lee, S., You, Y.H., 2014. A robust joint frequency offset estimation for the OFDM system using cyclic delay diversity. *Wireless Personal Communications*, 77(4), pp.2483-2496.

Sirvi, S., Tharani, L. *Wavelet based OFDM system over flat fading channel using NLMS equalization*. In: Proceeding International Conference on Computing, Communication and Automation (ICCCA), 2016.

Strang, G., 1999. The discrete cosine transform. *SIAM Review*, 41(1), pp.135-147.

Suma, M.N., and Narasimhan, S.V., 2018. Efficient analytic discrete cosine harmonic wavelet transform OFDM with denoising. *International Journal of Wireless and Mobile Computing*, 14(8), pp.223-228.

Tse, D., Viswanath, P., 2005. *Fundamentals of Wireless Communications*. New York: Cambridge University Press, 2005.

Wang, Z., Zhang, S., Qiu, B., 2010. PAPR Reduction of OFDM Signal by Using Hadamard Transform in Companding Techniques. 12th IEEE International Conference on Communication Technology, pp. 320-323.